

STOCHASTICALLY INDUCED GAMMA-RAY BURST WAKEFIELD PROCESSES

JACOB TRIER FREDRIKSEN

Stockholm Observatory, AlbaNova University Center, SE-106 91 Stockholm, Sweden

Submitted to Astrophysical Journal Letters.

ABSTRACT

We present a numerical study of Gamma-Ray Burst - Circumburst Medium interaction and plasma preconditioning via Compton scattering. The simulation tool employed here – the PHOTONPLASMA code – is a unique hybrid model; it combines a highly parallelized (Vlasov) particle-in-cell approach with continuous weighting of particles and a sub-Debye Monte-Carlo binary particle interaction framework. Our first results from 3D simulations with this new simulation tool suggest that magnetic fields and plasma density filaments are created in the wakefield of prompt gamma-ray bursts, and that the photon flux density gradient has a significant impact on particle acceleration in the burst head and wakefield. We discuss some possible implications of the circumburst medium preconditioning for the trailing afterglow, and also discuss which additional processes will be needed to improve future studies within this unique and powerful simulation framework.

Subject headings: Gamma rays: bursts – plasmas – magnetic fields – methods: numerical – instabilities – acceleration of particles

1. INTRODUCTION

The microphysics of Gamma-Ray Burst (GRB) afterglow shocks propagating through a circumburst medium (CBM) has been extensively studied using particle-in-cell (PIC) models in the past few years (see e.g. Keshet et al. 2008; Hededal et al. 2004; Frederiksen et al. 2004; Silva et al. 2003; Gruzinov 2001). In contrast, the initial interaction between the GRB photons and the CBM plasma is less well studied numerically, although progress has been made for coherent wakefield processes in lower-dimensional and pair plasmas (e.g. Hoshino 2008; Liang & Noguchi 2007). Whereas the burst-CBM interaction has received strong attention in theoretical (Beloborodov 2004, 2002; Thompson & Madau 2000) and observational (Connaughton 2002) works, the detailed microphysical plasma dynamics in the first pulse-plasma encounter lacks sufficient treatment with respect to the high degree of forcing anisotropy in the problem of photon scattering off the relatively cold tenuous CBM.

Wakefield interactions between high energy photon pulses and a plasma have been extensively studied in the context of *coherent* wakefield acceleration in laser-plasma systems, both experimentally (e.g. Phuoc et al. 2005; Kostyukov et al. 2003), and numerically in the same context (e.g. Phuoc et al. 2005; Pukhov 2000). In the astrophysical context of particle acceleration in GRBs, wakefield acceleration has been studied in the coherent regime where the forcing of the plasma is done by the electromagnetic field (Hoshino 2008; Liang & Noguchi 2007). Incoherent – or *stochastic* – wakefield processes have to our knowledge so far not been studied numerically, and has been considered theoretically only in a few cases (e.g. Barbiellini et al. 2006, 2004).

Our motivation for developing a new and improved Particle-in-cell- Monte-Carlo (PIC-MC) code framework for investigating the detailed Compton interaction of an ultra-intense GRB and a quiescent cold CBM is two-fold:

First, due to the high-energy spectrum of the prompt GRB (for BATSE of order $E_\gamma \sim m_e c^2$), the photon wavelength is much shorter than any characteristic length scale in the CBM plasma, $\lambda_\gamma \ll \delta_e$ and $\lambda_\gamma \ll \lambda_D$, with δ_e and λ_D the electron

skin-depth and Debye-length resp. We may therefore expect a binary approximation to work well for prompt burst photons interacting with the plasma constituent particles through Compton scattering. In fact, photons in a large range down towards the electron plasma frequency $\omega_\gamma \sim \omega_{pe} = \lambda_D^{-1} v_{th,e}$ (where $v_{th,e}$ is the electron thermal speed) could be treated as point particles that interact in a binary way with the plasma.

Secondly, the extreme intensity of the burst makes the GRB front opaque to the plasma electrons. Assuming a CBM with $n_e \approx 1 \text{ cm}^{-3}$ and typical WR wind temperatures, $T_e \approx 10^5 \text{ K}$, and further assuming a typical BATSE GRB with an estimated (from Barbiellini et al. 2006, eqn.2) photon flux energy density of $10^{25} \text{ eV cm}^{-2} \text{ s}^{-1}$ at distance $R_0 \sim 10^{16} \text{ cm}$ from the progenitor, Compton scattering of the CBM plasma electrons will occur at least once every second per electron during the prompt phase, whereas most photons survive traversing the plasma without being significantly affected. The plasma is forced predominantly by binary particle- particle encounters, everywhere locally.

These considerations motivated us to develop and employ a new and unique tool in order to gain access to the sub-Debye regime. Adopting the "random phase approximation" (Pines & Bohm 1952) we may split, in a natural way, plasma processes into two different numerical schemes depending on the characteristic scale of the dynamics, here denoted \mathbf{k}_C :

$\lambda_D \ll |\mathbf{k}_C|^{-1}$: for forcing and disturbances scale larger than the Debye length the Vlasov approach is applied and the PIC code framework is utilized.

$\lambda_D \gg |\mathbf{k}_C|^{-1}$: in the opposite case dynamics is particle-particle interaction dominated, and we solve the scattering problem statistically through MC radiative transfer for the plasma constituents.

In this way we obtain a substantially improved description of the plasma for both the Vlasov and detailed balance cases, and capture in a natural way the details of wave-particle interaction and scattering. The PHOTONPLASMA code is parallelized with MPI and is highly scalable, and any plasma

constituent species, forcing and scattering process is possible to incorporate with relative ease; for further details see (Frederiksen 2008; Haugboelle 2005). We are presently implementing photon-photon pair production, which will be incorporated in future numerical studies.

In the remainder of this Letter we present, in Section 2, some central details on our numerical approach, and account for the simulation setup as well as physical and numerical scaling. Results and discussion are given in Section 3, where we also relate the wakefield effects to other results concerning coherent – rather than stochastically induced – wakefield processes. Our conclusions and commentary on future ways to improve and expand the simulations are given in Section 4.

2. THE STOCHASTIC WAKEFIELD SIMULATION

Here we describe the 3D runs from our first wakefield experiments, full details of this as well as other setups, tests and more results can be found in Frederiksen (2008).

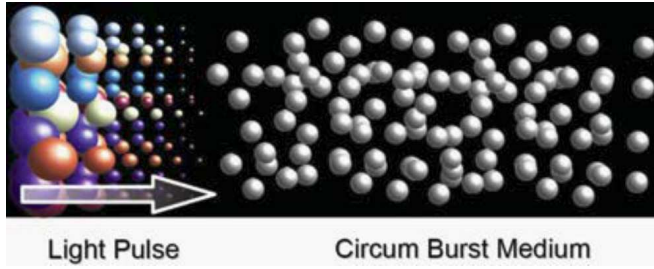


FIG. 1. — Illustration of the prompt flash traversing the circumburst medium for our computational model. The photons (left) are moving through the ambient CBM plasma, and as the intensity of the light pulse increases, the *weights* (size) of the photons vary, rather than the *number*. Color designates that photons carry different energies (through ν) as well. We save computational power and gain in speed. The microphysics is unchanged.

A synthetic thermal GRB is delivered to the quiescent CBM plasma by adding photons (particles) to the computational domain on a volume boundary, as illustrated in figure Fig. 1, according to a prescribed light curve and spectrum.

The light curve is inspired by BATSE data fitted to a FRED function (Ryde et al. 2003; Kocevski et al. 2003) with parameters chosen for BATSE trigger 3891, $r = 1.26$ and $d = 2.67$. The spectrum is assumed to be Planckian (black body): $N_\gamma(\nu, t) = (h\nu)^{-1} F(\nu, t) \equiv (h\nu)^{-1} B_\nu(T(t), t)$, for the photon spectral radiance. We use the Stefan-Boltzmann law to model the temperature, $T(t) \propto F(t)^{1/4}$. The spectral window coincides with the BATSE window, $E_\gamma \in [33.6\text{keV}, 3.36\text{MeV}]$ – after correction for an estimated redshift of $z \sim 1.68$ Ryde et al. (2003). Our FRED model has duration $\tau_{GRB} = 200$, which corresponds to about 1% of T_{50} for trigger 3891.

We evolve our synthetic GRB by adding a constant number of photons per cell carrying *continuous* weights prescribed by the FRED- Planckian burst functions. Photon energies are sampled from MC integration of the (time-dependent) Planckian – we thus obtain a comparatively high accuracy at low computational cost. The photon spectral radiance (spectral photon number density) is given by

$$n_\gamma(\nu, t) \propto \frac{F(\nu, t)}{\nu} \propto \sum_{i=1}^{N_\gamma(\nu, t)} w_i(\nu, t) \Rightarrow n_\gamma(\nu, t) \propto \sum_{i=1}^{N_\gamma(\nu)} w_i(t),$$

using our assumptions about the thermal GRB. The split into assigning time-variability to the weights and frequency vari-

ability to individual particles gives a high degree of flexibility compared to conventional PIC codes.

The CBM quiescent plasma is assumed to be a homogeneous uniform density medium, consisting of a hydrogenic, fully ionized, moderate temperature plasma with $v_{th,e} \approx 0.1c$. We have adopted conventional PIC scaling, setting all relevant natural constants equal to unity, except the ion-to-electron mass ratio which we have set to $m_i/m_e = 256$. The initial number of particles per cell is 40/ species, and the grid resolution $100 \times 20 \times 4000$, which translates to $\{L_x, L_y, L_z\} \approx \{13\delta_e \times 2\delta_e \times 500\delta_e\}$ for our choices of length units and plasma density. The burst duration in light travel length is $L_{GRB} \approx 64\delta_e$.

The choice of a relatively flat volume aspect ratio is a compromise to ensure skin-depth resolution at the lowest possible grid size to give any 3D structure a chance of growing marginally without spending excess computing time. Boundary conditions are for the lower (upper) boundaries: plasma particles are specularly reflected (thermalized) and outgoing photons are removed. Fields are damped in a layer $\Delta L_z \sim 0.1\% L_z$ on the boundaries to avoid spurious wave- interference.

Compton scattering interaction between photons and plasma electrons is conducted through MC detailed balance binary scattering. Photons and electrons are selected pairwise at random for scattering according to their weights. We use the full Klein-Nishina expression for the micro-physical scattering. The scattering is done by splitting the particles into a new part carrying the Compton scattered fraction of the old part (Haugboelle 2005), and an unscattered remaining part. We may write

$$W_{(\gamma,e),scatt} = W_{(\gamma,e),old} - W_{(\gamma,e),new}, \quad W_{e,\gamma} \in \mathbb{R}^+,$$

where the number (weight) of scattered electrons and photons are equal pairwise, by definition. The fraction of scattered particles per time step then satisfies

$$W_{(e,\gamma),scatt} \propto W_e W_\gamma \overline{\sigma}_C(\mathbf{p}_e, \mathbf{p}_\gamma) c \Delta t,$$

where $\overline{\sigma}_C(\mathbf{p}_e, \mathbf{p}_\gamma)$ denotes the microphysical Compton scattering matrix for photons and electrons in a given cell. Effectively, for a scattering fraction of 10^{-6} , 10^{24} *physical* particles are scattered away from a ‘mother’ particle of size 10^{30} , for example; this illustrates the flexibility and the fundamentally continuous nature of the PHOTONPLASMA code.

3. RESULTS AND DISCUSSION

3.1. Wakefield-Plasma Gradient Effects and Transients

As the pulse interacts with the quiescent plasma, electrons are strongly forward Compton scattered. The plasma reacts electrostatically to restore the displacement by pulling the bulk of the electrons backwards anti-parallel to the burst propagation direction, while this in turn back-reacts on the photons. The effects can be seen as the ‘dip’ from $z = 1500$ backwards (to the left) in figures 2 and 3, where scatter plots in plasma sub-phase space $\{z, |\mathbf{p}_z|\}$ are shown for electrons and photons, respectively. The scatter plots are from runs with twice the resolution and half the density of those for the main simulation (described in Section 2). The well resolved and longer skin depth reveals strong electrostatic beating in the plasma parallel momentum. These beats lasts of order $\tau_b \sim \delta_e/c \sim 10^{-4}\text{s}$ in the CBM rest frame, and particles caught in the wake reach Lorentz factors upward of $\gamma_e \sim 40$.

Forwardly accelerated plasma – above the yellow line in Fig. 2 – relaxes to $|p_{z,e}| \sim \pm m_e c$ in a pace proportional to the

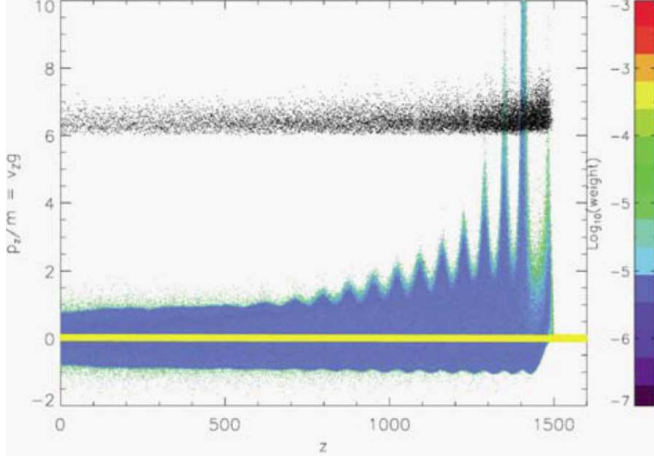


FIG. 2.— *Electron Scatter Plot*: Color designates weight in log-scale – blue particles have weights $w_{blue} \sim 10^{-5}w_0$, where w_0 is the initial weight. The yellow line coincides with zero bulk z -momentum, $p_{z,\gamma} = 0$. For clarity photons (black) are offset vertically by $p_{z,\gamma} = +6$.

burst duration, in order to counter-act the bulk backwards flow initiated by the photons. The plasma undergoes violent deceleration, in order to not compromise charge-neutrality. Burst photons keep the electron population ‘inflated’ as long as photon free energy and anisotropy is available in the plasma; far downstream the ‘inflated’ non-thermal population lasts through the duration of our simulations.

The violent electrostatic acceleration of plasma electrons, due to the sharp gradient in photon pressure, will produce bremsstrahlung and synchrotron photons, and subsequently upscattered these will eventually affect the spectrum (Barbiellini et al. 2006). More importantly, millisecond variability could – in our assumed environment – arise directly from the enhanced density variations, scattering and possibly pair production (leading to higher densities and more scattering). Such a variability, which is comparable to the plasma frequency in a medium with density $n_0 \sim 10^{-1}\text{cm}^{-3} - 10^0\text{cm}^{-3}$, could therefore be self-feeding and grow in strength and duration. We may be observing the weak seed to such a spike in the spectrum at high energy, marked by the two pink arrows in Fig. 3. Integrated over some fraction of the burst duration, such spikes could resemble a high-energy tail in the spectrum.

3.2. Magnetic Field Generation

Most intriguingly, we observe growth of a strong, large-scale magnetic field in the downstream wakefield gradient region. The entire scenario is captured in Fig. 4. A cross section of the 3D volume is shown for electrons, photons, ions and the transverse magnetic field, B_\perp (top-to-bottom), for the 3D run described in Section 2. Barely visible in the electron population is the same electrostatic spiky structure that shows in Fig. 2, but somewhat weaker due to comparatively higher density and lower resolution.

As is seen from the panels for ion density and electron density, both species undergo instability in the same way, as they tend to form confluent filaments in the plasma (although the inertia difference plays a role). The filamentation and current channel build-up is created by a stochastically induced electrostatic field gradient from fluctuating EM fields in front of the burst. These give rise to an effective ponderomotive force $\mathbf{F}_p \propto -q_e^2(m\omega)^{-1}\nabla E^2$, which is independent of

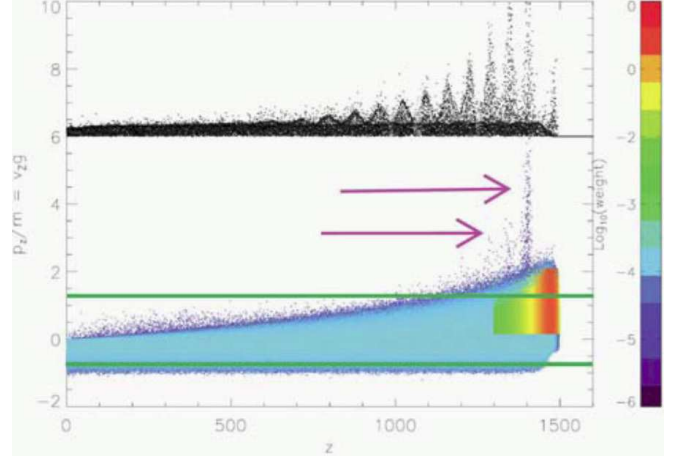


FIG. 3.— *Photon Scatter Plot*: same run as Fig. 2, but for photons (in color). The initial burst (moving right) is visible from $t \sim 1500$ to $t \sim 1300$. Pink arrows: local photon upscattering. Green lines: energy threshold for $\gamma + \gamma \rightarrow e^+ + e^-$ for photons pairwise oppositely outside (away from $p_z = 0$) these lines. Electrons (black) are offset by $p_{z,e} = +6$. Here, $p_{z,\gamma} \equiv [h\nu]_z/m_e c^2$.

the charge *sign*. Consequently both electrons and ions drift in the same manner. The effect is self-sustaining as long as the photon momentum anisotropy is sufficiently high. This instability has also been identified by other authors (Hoshino 2008; Liang & Noguchi 2007) as being responsible for the acceleration of particles due to intense forcing by precursor Poynting flux pulses. The coherent nature of the plasma forcing, however, contrasts our stochastic forcing leading to field generation. It remains to be determined whether such a field will also grow in a field driven environment.

Determining the rate with which the magnetic field decays on very long time scales is a challenge yet to be met. Modeling a larger plasma volume is necessary to determine the ultimate temporal and spatial development. Resorting to lower-dimensional models will not solve the problem – we argue that this instability is inherently 3D in nature and cannot be followed reasonably beyond the linear regime of the fastest growing instability, (cf. Frederiksen et al. 2004; Frederiksen 2008).

We notice from observing Fig. 4 that filaments, current structures and field scales are limited by the computational volume – i.e. they are ‘boxed-in’. Nonetheless, they survive relatively far behind the final tail of the photon wakefield (the GRB), both electrons and ions are responsible for the density filaments, the current densities are borne almost entirely by the electrons – again – owing to the inertial difference. We may therefore expect that as long as the photon anisotropy is “large”, the field structures will survive. We note that our synthetic GRB comprises only a small frequency window and cannot continue to feed the plasma as effectively as would a real burst spanning a much larger range of frequencies for a longer time.

We proceed to speculate that such a field could provide a magnetic ‘wall’ against which trailing ejecta could gradually produce a build-up of shocks and particle acceleration, as the ejecta traverses the pre-conditioned circumburst medium.

4. CONCLUSIONS

We emphasize the importance of bridging the gap between the (statistical) sub-Debye domain and the macroscopic Vlasov-/super-Debye domain in astrophysical plasma modeling, opening the possibility of a detailed kinetic photon de-

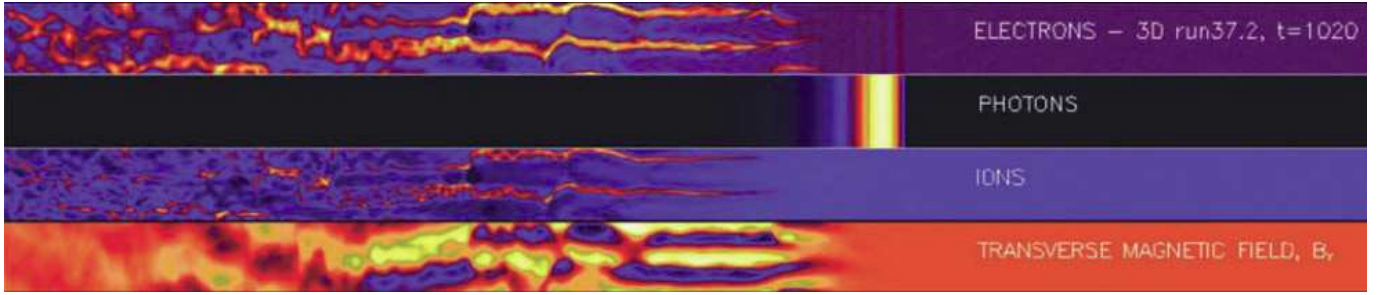


FIG. 4.— Current structures for electrons (panel 1), photon pulse (panel 2), ions (panel 3) and (transverse, out-of-plane) magnetic field structure (panel 4) in our 3D wakefield simulation, at simulation time $t = 1020\omega_{pe}^{-1} \approx 10^4 \Delta t$. The GRB photon pulse has light-length $L_c \equiv c/\tau_{GRB} = 200 \approx 64\delta_e$. The computational volume has dimensions $\{L_x, L_y, L_z\} = \{40, 8, 1600\}$ or, in electron skin-depths, $\{L_x, L_y, L_z\} \approx \{12\delta_e, 2\delta_e, 500\delta_e\}$.

scription, and allowing the modeling of processes such as neutron transport and decay, neutrino streaming and transport, pair production etc.

Frequencies for wave-particle collisions *versus* particle-particle collisions (e.g. Compton) are vastly different in magnitude for the physical conditions we have considered in this Letter. Generally, here, the effective “collisions rate” due to wave-particle interaction is several orders of magnitude higher than the rate of Compton scattering. In effect

$$\nu_{\text{coll}} \propto \omega_{pe} = c^{-1} \delta_e, \quad \nu_{\text{bin}} \propto n c \sigma_T \Rightarrow \nu_{\text{coll}} \gg \nu_{\text{bin}},$$

where n is the photon number density, σ_T the Thompson cross section, l the burst light duration. Subscripts “coll” and “bin” denote “collective” (wave-particle), and “binary” (particle-particle) - respectively. We have approximated the Compton collision frequency from simple mean free path argument; $l_{mfp} \sim (n\sigma c)^{-1}$.

The violent acceleration of electrons in the wakefield (see Fig. 2) leads to the need to assess the spectra that arise from such accelerated electron populations (Hededal 2005). This functionality has recently been incorporated as a fully dynamic runtime spectral synthesizer module, capable of collecting the spectral data while concurrently evolving the plasma fields and sub-Debye components of the PHOTON-PLASMA code as well.

It has been argued theoretically (Beloborodov 2002; Thompson & Madau 2000) that the CBM ahead of the trailing forward shock could be loaded with a relatively high density pair plasma component. From this work, and from observing Fig. 3, we see that accounting for pair production ($\gamma + \gamma \leftrightarrow e^+ + e^-$) is imperative, a project which we are cur-

rently entertaining.

Our main findings from these first simplified GRB-CBM wakefield interaction simulations, which we have conducted with the new PHOTONPLASMA hybrid scheme described briefly in Section 2, are:

1. Strong photon density gradients plays an important role in the dynamics of the CBM while being traversed by a GRB. We therefore lend support from our studies to suggestions set forth by (Barbiellini et al. 2006) to study in more detail these stochastically induced wakefield processes.
2. The GRB spectrum is locally affected by the same gradient density induced effects, and this leads to local high energy fluctuations in the GRB spectrum and light curve on sub-millisecond-to-millisecond time scales.
3. A relatively strong transverse magnetic field, quasi-static in the CBM frame, is generated in the wakefield of a GRB traversing a quiescent plasma. The field scales grow beyond our numerical capabilities to follow the growth.

In future work we will add pair dynamics, to test in particular whether this might create density fluctuations that could grow and eventually lead to externally produced shocks as a consequence of γ -ray preconditioning of the circumburst medium.

Collaboration with Troels Haugbølle, Christian Hededal, and Åke Nordlund on the development of the PHOTON-PLASMA code is acknowledged. Computer time was provided by the Danish Center for Scientific Computing (DCSC).

REFERENCES

- Barbiellini, G., Celotti, A., Ghirlanda, G., Longo, F., Piro, L., & Tavani, M. 2004, MNRAS, 350, L5
- Barbiellini, G., Longo, F., Omodei, N., Celotti, A., & Tavani, M. 2006, in American Institute of Physics Conference Series, Vol. 836, Gamma-Ray Bursts in the Swift Era, ed. S. S. Holt, N. Gehrels, & J. A. Nousek, 91–96
- Beloborodov, A. M. 2002, ApJ, 565, 808
- Beloborodov, A. M. 2004, in American Institute of Physics Conference Series, Vol. 727, Gamma-Ray Bursts: 30 Years of Discovery, ed. E. Fenimore & M. Galassi, 187–191
- Connaughton, V. 2002, ApJ, 567, 1028
- Frederiksen, J. T. 2008, PhD thesis, Stockholm Observatory
- Frederiksen, J. T., Hededal, C. B., Haugbølle, T., & Nordlund, Å. 2004, ApJ, 608, L13
- Gruzinov, A. 2001, ArXiv Astrophysics e-prints, astro-ph/0111321
- Haugboelle, T. 2005, ArXiv Astrophysics e-prints, astro-ph/0510292
- Hededal, C. 2005, PhD thesis, Niels Bohr Institute, astro-ph/0506559
- Hededal, C. B., Haugbølle, T., Frederiksen, J. T., & Nordlund, Å. 2004, ApJ, 617, L107
- Hoshino, M. 2008, ApJ, 672, 940
- Keshet, U., Katz, B., Spitkovsky, A., & Waxman, E. 2008, ArXiv e-prints, astro-ph/0802.3217
- Kocevski, D., Ryde, F., & Liang, E. 2003, ApJ, 596, 389
- Kostyukov, I., Kiselev, S., & Pukhov, A. 2003, Physics of Plasmas, 10, 4818
- Liang, E., & Noguchi, K. 2007, ArXiv e-prints, astro-ph/0704.1843
- Phuoc, K. T., Burgi, F., Rousseau, J.-P., Malka, V., Rousse, A., Shah, R., Umstadter, D., Pukhov, A., & Kiselev, S. 2005, Physics of Plasmas, 12, 023101
- Pines, D., & Bohm, D. 1952, Phys. Rev., 85, 338
- Pukhov, A. 2000, Journal of Plasma Physics, 61, 425
- Ryde, F., Kocevski, D., & Liang, E. 2003, in American Institute of Physics Conference Series, Vol. 662, Gamma-Ray Burst and Afterglow Astronomy 2001: A Workshop Celebrating the First Year of the HETE Mission, ed. G. R. Ricker & R. K. Vanderspek, 286–288
- Silva, L. O., Fonseca, R. A., Tonge, J. W., Dawson, J. M., Mori, W. B., & Medvedev, M. V. 2003, ApJ, 596, L121
- Thompson, C., & Madau, P. 2000, ApJ, 538, 105